Solid-State Structures and Enzymatic Degradabilities for Melt-Crystallized Films of Copolymers of (*R*)-3-Hydroxybutyric Acid with Different Hydroxyalkanoic Acids

Hideki Abe and Yoshiharu Doi*

Polymer Chemistry Laboratory, The Institute of Physical and Chemical Research (RIKEN), Hirosawa, Wako-shi, Saitama 351-01, Japan

Hiromichi Aoki and Takashi Akehata

Department of Industrial Chemistry, Science University of Tokyo, 1−3, Kagurazaka, Shinjuku-ku, Tokyo 162, Japan

Received October 23, 1997; Revised Manuscript Received January 21, 1998

ABSTRACT: The films of random copolymers of (*R*)-3-hydroxybutyric acid with different hydroxyalkanoic acids such as (*R*)-3-hydroxypentanoic acid, (*R*)-3-hydroxyhexanoic acid, 4-hydroxybutyric acid, 6-hydroxyhexanoic acid, and (*S,S*)-lactide were prepared by the melt-crystallized method at various crystallization temperatures. The solid-state structures and thermal properties of melt-crystallized films were characterized by means of wide-angle X-ray diffraction, small-angle X-ray scattering, differential scanning calorimetry, optical microscopy, and scanning electron microscopy. Both the long period distance and the lamellar thickness of melt-crystallized polyester films were increased with an increase in the crystallization temperature. The melting temperature of polyester films also increased with an increase in the crystallization temperature. From the relationship between lamellar thickness and melting temperature, it has been concluded that randomly distributed second monomer units except for the (*R*)-3-hydroxypentanoic acid unit in copolyesters act as defects of poly[(*R*)-3-hydroxybutyric acid] crystal and are excluded from the crystalline lamellae. The enzymatic degradation of melt-crystallized films was carried out at 37 °C in an aqueous solution (pH 7.4) of PHB depolymerase from *Alcaligenes faecalis*. After enzymatic degradation, the smooth and rough planes were observed mutually along the radial direction of spherulites on the surface of melt-crystallized films, suggesting that PHB depolymerase predominantly hydrolyzes polymer chains on the edges of crystalline lamellar stacks. The enzymatic erosion rate of crystalline region in polyester films decreased with an increase in the lamellar thickness.

Introduction

The microbial poly(hydroxyalkanoic acid)s (PHA) family of polyesters is biodegradable thermoplastic produced from various carbon substrates by a number of bacteria.[1−3] The PHA has been shown to be formed as a storage material in over 90 genera of bacteria, and 91 different constituents of PHA have been identified as various hydroxyalkanoic acids with three to fourteen carbon atoms.[4] These biodegradable PHA polymers have attracted much attention as environmentally degradable thermoplastics to be used for a wide range of agricultural, marine, and medical applications.[1] A remarkable characteristic of PHA is their biodegradability in various environments.[1,2] A number of microorganisms such as bacteria and fungi in environments excrete PHB depolymerases to hydrolyze the solid PHA into water-soluble oligomers and monomer, and they utilize the resulting products as nutrients within cells. Aerobic and anaerobic PHA-degrading microorganisms have been isolated from various ecosystems, and the properties of their extracellular PHB depolymerases have been studied.[5−7] Analysis of the primary structure revealed that the enzymes of 393−488 amino acids are composed of two functional domains and a region linking the two domains. One is a catalytic domain containing the catalytic triad of serine, aspartate, and histidine, while the other is a substrate-binding domain which adsorbs on the surface of partially crystalline P[(*R*)-3HB] and orients the catalytic domain toward the substrate.

In previous papers,[8−12] we have studied the enzymatic degradation of the solvent-cast films of various PHA copolymers in the presence of PHB depolymerase from *Alcaligenes faecalis* and reported the effects of chemical structure of second monomer units and copolymer compositions on the rate of enzymatic erosion. The rate of enzymatic erosion on the solvent-cast PHA films increased markedly with an increase in the fraction of second monomer units to reach a maximum value followed by a decrease in the erosion rate. The highest rates of enzymatic erosion were observed at 10−20 mol % of second monomer fraction for various PHA films, and the values were 5−10 times larger than the rate for the P[(*R*)-3HB] homopolymer film. The water-soluble products during the enzymatic degradation of PHA films were a mixture of monomer and oligomers of hydroxyalkanoic acid units, suggesting that the PHB depolymerase acts as an *endo*-type hydrolase toward polyester chains.

The melt-crystallized films of P[(*R*)-3HB] exhibit large spherulites of diameter 50−500 μm, and the spherulitic morphology and degree of crystallinity are dependent on the crystallization conditions.[13,14] Kumagai et al. [15] reported that the rate of enzymatic hydrolysis of melt-crystallized P[(*R*)-3HB] film by PHB depolymerase from *A. faecalis* decreased with an increase in the crystallinity of P[(*R*)-3HB] film, while that the size of spherulites did not affect the rate of hydrolysis. Recently,

* Author to whom correspondence should be addressed.

S0024-9297(97)01559-3 CCC: $15.00
Published on Web 03/05/1998

Table 1. Molecular Weights and Glass-Transition Temperatures of Eight Polyester Samples

sample	molecular weight		glass-transition temperature (T_g), °C
	$M_n \times 10^{-3}$	M_w/M_n	
P[(*R*)-3HB]	300	2.3	4
P[(*R*)-3HB-*co*-6 mol % (*R*)-3HV]	183	2.4	0
P[(*R*)-3HB-*co*-16 mol % (*R*)-3HV]	130	2.6	2
P[(*R*)-3HB-*co*-8 mol % (*R*)-3HH]	279	2.4	0
P[(*R*)-3HB-*co*-8 mol % 4HB]	197	1.9	−4
P[(*R*)-3HB-*co*-10 mol % 4HB]	47	1.9	−5
P[(*R*)-3HB-*co*-10 mol % 6HH]	107	1.7	−5
P[(*R*)-3HB-*co*-5 mol % LA]	91	1.8	8

Tomasi et al. [16] reported that the rate of enzymatic erosion of melt-crystallized P[(*R*)-3HB] films with PHB depolymerase from *Pseudomonas lemoignei* decreased with an increase in the average size of P[(*R*)-3HB] crystals. More recently, Koyama and Doi [17] studied the enzymatic degradabilities of melt-crystallized films of various PHA copolymers by PHB depolymerase from *A. faecalis* and reported that the erosion rates for poly[(*R*)-3-hydroxybutyric acid-*co*-7 mol % (*R*)-3-hydroxypentanoic acid] films were several times higher than the rates of P[(*R*)-3HB] homopolymer films with the same degree of crystallinity. These reported results prompted us to investigate the effect of lamellar crystal structure on the enzymatic degradability of PHA films.

In this paper, we study the thermal properties and solid-state structures for melt-crystallized films of biosynthetic and chemosynthetic copolymers of (*R*)-3HB with various hydroxyalkanoic acids. In addition, the rates of enzymatic erosion of melt-crystallized PHA films are measured in the presence of PHB depolymerase from *A. faecalis*, and the effects of solid-state structures on the rate of enzymatic erosion are discussed.

Experimental Section

Materials. Poly[(*R*)-3-hydroxybutyric acid] (P[(*R*)-3HB]) homopolymer[18] and three types of copolyesters; poly[(*R*)-3-hydroxybutyric acid-*co*-(*R*)-3-hydroxypentanoic acid] (P[(*R*)-3HB-*co*-(*R*)-3HV]),[10] poly[(*R*)-3-hydroxybutyric acid-*co*-(*R*)-3-hydroxyhexanoic acid] (P[(*R*)-3HB-*co*-(*R*)-3HH]),[10] and poly[(*R*)-3-hydroxybutyric acid-*co*-4-hydroxybutyric acid] (P[(*R*)-3HB-*co*-4HB]),[19] were prepared by microbial synthetic methods. Poly[(*R*)-3-hydroxybutyric acid-*co*-6-hydroxyhexanoic acid] (P[(*R*)-3HB-*co*-6HH])[11] and poly[(*R*)-3-hydroxybutyric acid-*co*-(*S*,*S*)-lactide] (P[(*R*)-3HB-*co*-LA])[12] were synthesized by the ring-opening copolymerization of (*R*)-β-butyrolactone (e.e. 92%) with ϵ-caprolactone or (*S*,*S*)-lactide in the presence of tin-based catalyst. The number-averaged molecular weights (M_n), polydispersities (M_w/M_n), and glass-transition temperatures (T_g) of eight PHA samples used in this study are listed in Table 1. By analysis of the ^{13}C nuclear magnetic resonance (NMR) spectra of copolyesters, the sequence distributions of (*R*)-3HB and other hydroxyalkanoic acid units in all copolyesters were found to be statistically random.[8−12]

Preparation of Melt-Crystallized Films. All films were initially prepared by conventional solvent-cast techniques from chloroform solutions of polyesters using glass Petri dishes as casting surfaces. Solvent-cast films were inserted between two Teflon sheets with a Teflon sheet (0.05 mm thickness) as a spacer and were compression-molded on a Mini Test Press (Toyoseiki) by heating at 200 °C for 1 min under a pressure of 75 kg/cm^2. After melting, samples were kept at a given crystallization temperature (T_c) and isothermally crystallized for 3 days.

Enzymatic Degradation Test. The extracellular PHB depolymerase was purified to electrophoretic homogeneity from *A. faecalis*.[20] The enzymatic degradation of melt-crystallized PHA films was carried out at 37 °C in 0.1 M potassium phosphate buffer (pH 7.4). Films (initial weights, about 6 mg; initial dimensions, 10 × 10 × 0.05 mm) were placed in small glass bottles containing 1.0 mL of phosphate buffer. The reaction was started by the addition of 2.6 μL of an aqueous solution of PHB depolymerase (1.0 μg). For the weight loss measurement of identical film sample, at least five reaction solutions were prepared and incubated at 37 ± 0.1 °C with shaking. One sample film was removed after a given reaction time, washed with distilled water, and dried to constant weight in vacuo before analysis. From the values of weight loss for five films immersed in reaction solutions for different periods, a plot of weight loss against reaction time was obtained.

Analytical Procedures. Differential scanning calorimetry (DSC) data of PHA films were recorded in the temperature range 0−200 °C on a Shimadzu DSC-50Q equipped with a cooling accessory under a nitrogen flow of 30 mL/min. Samples of 3 mg were encapsulated in aluminum pans and heated from 0 to 200 °C at a rate of 20 °C/min. The melting temperature (T_m) and enthalpy of fusion (ΔH_m) were determined from the DSC endotherms. The T_m was taken as the peak temperature.

The wide-angle X-ray diffraction patterns of films were recorded at 27 °C on a Rigaku RAD-IIIB system using nickel-filtered Cu Kα radiation ($\lambda = 0.154$ nm; 40 kV; 30 mA) in the 2θ range 6−60° at a scan speed of 3.0°/min. Degrees of crystallinity (X_c) of PHA films were calculated from diffracted intensity data according to Vonk's method.[21] The small-angle X-ray scattering analyses of films were carried out at 27 °C using a Rigaku RINT 2500 system in the 2θ range 0.1−3.0° at a scan speed of 0.05°/min. Radiation of wavelength 0.154 nm (Cu Kα) was employed at a generator power of 40 kV and 200 mA.

The surface appearances of films were obtained with a scanning electron microscope (JEOL JSM-T220) after gold coating of melt-crystallized PHA films using an ion coater. Morphologies of melt-crystallized PHA films were observed with an optical microscope (Nikon OPTIPHOTO-2) equipped with a phase contrast lens.

Results and Discussion

Solid-State Structures of Melt-Crystallized Polyester Films. Melt-crystallized films of polyesters; P[(*R*)-3HB], P[(*R*)-3HB-*co*-6 mol % (*R*)-3HV], P[(*R*)-3HB-*co*-16 mol % (*R*)-3HV], P[(*R*)-3HB-*co*-8 mol % (*R*)-3HH], P[(*R*)-3HB-*co*-8 mol % 4HB], P[(*R*)-3HB-*co*-10 mol % 4HB], P[(*R*)-3HB-*co*-10 mol % 6HH], and P[(*R*)-3HB-*co*-5 mol % LA], were prepared by isothermal crystallization at different temperatures of 30−140 °C for 3 days from the melt at 200 °C for 1 min. After a crystallization period of 3 days, all polyester films showed the well-developed and volume-filled spherulites.

The crystalline structure of melt-crystallized polyester films was characterized by wide-angle X-ray diffraction analysis. The diffraction patterns of all melt-crystallized samples showed reflections arising from the crystalline lattice of P[(*R*)-3HB]. The X-ray crystallinities of polyester films were calculated from the diffraction patterns, and the data are listed in Table 2. The crystallinity of melt-crystallized polyester films ranged from 34 to 78%.

The thermal properties of melt-crystallized polyester films was characterized by differential scanning calorimetry (DSC), and all data are listed in Table 2. Figure 1 shows the typical DSC curves of P[(*R*)-3HB-*co*-10 mol % 6HH] film crystallized at 80 °C recorded at defferent heating rates. Two endothermic peaks were detected in the thermograms for several copolyester samples. To examine whether the peak at high-temperature arises from a recrystallization process, the DSC curves of melt-crystallized films were recorded at different heating

Table 2. Thermal Properties, Solid-State Structures, and Rates of Enzymatic Erosion for Melt-Crystallized Polyester Films[a]

sample	crystallization temp (T_c), °C	melting temp (T_m), °C		heat of fusion (ΔH_m), J/g	X-ray crystallinity (X_c), %	long period (L_p), nm	lamellar thickness (l_c), nm	rate of erosion, mg/(h·cm^2)
P[(*R*)-3HB]	60	166		99	65 ± 5	7.4	5.3	0.049 ± 0.002
	90	169		110	63 ± 5	8.4	5.8	0.066 ± 0.002
	100	171		116	70 ± 5	9.2	6.2	n.d.
	110	173		n.d.	78 ± 5	9.9	6.8	0.033 ± 0.003
	120	175		122	70 ± 5	10.2	6.5	0.037 ± 0.001
	130	177		122	70 ± 5	12.1	8.2	0.027 ± 0.001
	140	180		n.d.	72 ± 5	n.d.	n.d.	0.016 ± 0.001
P[(*R*)-3HB-*co*-6 mol % (*R*)-3HV]	60	151	162	71	61 ± 4	7.2	4.1	0.220 ± 0.018
	80	154	162	71	67 ± 5	8.1	5.5	0.172 ± 0.015
	90	157		75	68 ± 6	9.0	6.1	0.101 ± 0.011
	100	159		73	65 ± 5	9.3	6.1	0.111 ± 0.013
	110	161		73	71 ± 5	10.1	5.8	0.070 ± 0.009
	120	164		71	66 ± 4	11.9	6.3	0.067 ± 0.004
	130	169		74	73 ± 6	13.8	8.5	0.050 ± 0.004
P[(*R*)-3HB-*co*-16 mol % (*R*)-3HV]	40	133	149	66	63 ± 5	6.7	4.0	n.d.
	60	138	150	64	61 ± 5	7.4	4.6	0.472 ± 0.051
	70	139	152	72	64 ± 6	n.d.	n.d.	0.322 ± 0.032
	80	142	153	71	65 ± 6	10.3	6.0	n.d.
	90	146		74	61 ± 4	12.6	7.3	0.345 ± 0.031
	100	149		72	62 ± 5	13.4	7.5	0.212 ± 0.019
	105	152		71	65 ± 5	n.d.	n.d.	0.208 ± 0.019
	110	154		72	64 ± 4	16.7	9.0	0.307 ± 0.029
	120	155		70	70 ± 6	17.1	10.8	0.321 ± 0.033
P[(*R*)-3HB-*co*-8 mol % (*R*)-3HH]	60	121	137	59	55 ± 5	6.4	1.9	0.170 ± 0.011
	70	125	138	62	54 ± 5	7.3	2.0	0.151 ± 0.011
	80	127	138	66	58 ± 4	7.4	2.1	0.156 ± 0.013
	90	128		69	55 ± 5	8.2	2.3	n.d.
P[(*R*)-3HB-*co*-8 mol % 4HB]	60	132	149	69	57 ± 5	7.2	2.2	0.386 ± 0.042
	80	139	154	68	62 ± 6	7.3	2.3	0.276 ± 0.022
	90	141	154	68	60 ± 4	8.1	2.4	0.161 ± 0.013
	100	146		57	62 ± 4	9.2	3.3	0.150 ± 0.015
	110	149		68	64 ± 5	9.9	3.5	0.116 ± 0.009
	120	154		72	63 ± 6	n.d.	n.d.	0.085 ± 0.009
P[(*R*)-3HB-*co*-10 mol % 4HB]	30	113	134	62	50 ± 4	5.3	1.9	n.d.
	50	119	137	57	59 ± 5	6.6	2.1	0.328 ± 0.033
	60	122	138	62	56 ± 5	7.4	2.1	0.370 ± 0.031
	70	124	138	57	60 ± 6	7.4	2.1	0.369 ± 0.029
	85	132		65	62 ± 5	7.6	2.3	0.140 ± 0.020
	90	134		67	65 ± 6	7.8	2.4	0.158 ± 0.011
	95	136		68	65 ± 4	7.9	2.4	0.143 ± 0.013
P[(*R*)-3HB-*co*-10 mol % 6HH]	30	102	130	53	34 ± 3	6.4	1.6	n.d.
	40	106	131	56	43 ± 3	n.d.	n.d.	n.d.
	50	110	131	57	40 ± 4	7.2	1.7	0.840 ± 0.051
	60	112	131	60	43 ± 4	7.3	1.8	0.790 ± 0.068
	65	115	131	50	47 ± 3	n.d.	n.d.	0.570 ± 0.048
	70	116	131	69	50 ± 4	8.2	1.8	0.580 ± 0.056
	75	120	132	55	48 ± 4	n.d.	n.d.	0.425 ± 0.055
	80	119	133	64	43 ± 5	9.0	1.9	0.396 ± 0.036
	85	122	133	70	48 ± 5	n.d.	n.d.	0.515 ± 0.041
	90	124	134	56	45 ± 4	8.3	2.3	0.406 ± 0.048
	95	126	34	57	44 ± 4	n.d.	n.d.	0.487 ± 0.036
	100	128		69	44 ± 4	8.2	2.2	0.575 ± 0.062
	105	129		62	44 ± 5	n.d.	n.d.	0.487 ± 0.047
	110	130		60	47 ± 5	8.2	2.2	0.405 ± 0.038
P[(*R*)-3HB-*co*-5 mol % LA]	60	126	138	65	52 ± 5	7.2	2.0	0.348 ± 0.022
	80	132	139	79	55 ± 4	7.5	2.3	0.203 ± 0.016
	90	135	141	76	58 ± 4	8.2	2.4	0.121 ± 0.009
	100	139		74	55 ± 5	8.3	2.7	0.109 ± 0.008
	110	142		69	51 ± 5	9.2	2.7	0.108 ± 0.010

[a] Key: n.d., not determined.

rates of 5−40 °C/min. As the heating rate was increased, the higher temperature peak became smaller while the lower temperature peak area increased (as shown in Figure 1). The result indicates that the higher melting endothermic peak is caused by the rearrangement of an initial crystal morphology of copolyester. The lower melting temperature represents the melting of original crystals formed at a crystallization temperature, and the value increased with crystallization temperature, suggesting that the thickness of crystalline lamellae in melt-crystallized polyester films increases with an increase in the crystallization temperature.

The enthalpies of fusion (ΔH_m) for melt-crystallized copolyester films were determined from the DSC curves. The melting endotherm apparently started from two different temperatures of room and crystallization temperatures. A high onset temperature of melting was observed at temperature of 10−15 °C above a crystallization temperature. Then, the enthalpy of fusion was determined from the high onset temperature of melting,

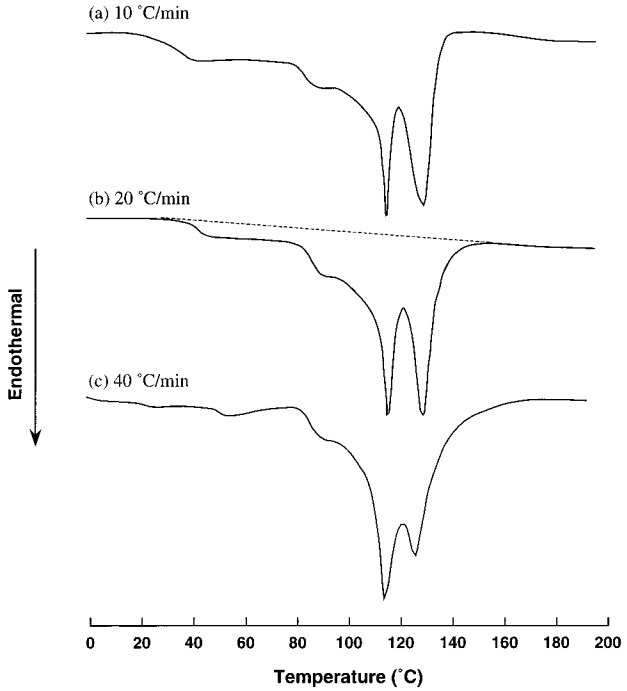

Figure 1. Typical DSC thermograms of P[(*R*)-3HB-*co*-10 mol % 6HH] film crystallized at 80 °C, recorded at heating rates of (a) 10, (b) 20, and (c) 40 °C/min.

and the value decreased with crystallization temperature (data not shown). On the other hand, the X-ray crystallinity of film increased with crystallization temperature, as shown in Table 2. It is of importance to note that overall melting endotherm has started from room temperature in the DSC curve. As it is shown in Table 2, overall enthalpy of fusion (ΔH_m) from the onset of melting at room temperature increased with crystallization temperature, and the relative crystallinity of film calculated from the overall enthalpy of fusion value was in good agreement with the value of X-ray crystallinity of films. During the primary crystallization process at a given crystallization temperature, relatively long sequences of (*R*)-3HB units in a random copolyester may be crystallized in P[(*R*)-3HB] crystalline lamellae, while shorter sequences of (*R*)-3HB units may remain in the amorphous region, resulting in the formation of relatively thick crystals. In this study, melt-crystallized films were allowed to stand at room temperature before analytical measurements. Then, relatively thin crystalline lamellae may be formed from shorter sequences of (*R*)-3HB units during the following crystallization process at room temperature. As a result, the melting endotherm may start from two different temperatures.

The lamellar structure of melt-crystallized polyester films were characterized by the small-angle X-ray scattering (SAXS) technique. Figure 2 shows a typical variation in relative SAXS intensities as a function of the magnitude of the scattering vector q for the samples of P[(*R*)-3HB-*co*-6 mol % (*R*)-3HV]. The scattering vector magnitude is defined by $q = 4\pi(\sin\theta)/\lambda$, where θ is half the scattering angle and λ is the wavelength of the radiation. To estimate the long period distance (L_p) and lamellar thickness (l_c) of the melt-crystallized polyester samples, the scattering data were analyzed according to the pseudo-two-phase model using a one-dimensional correlation function which can be taken directly as the Fourier transform of the scattering intensity.[22,23] The long period distance (L_p) and lamellar

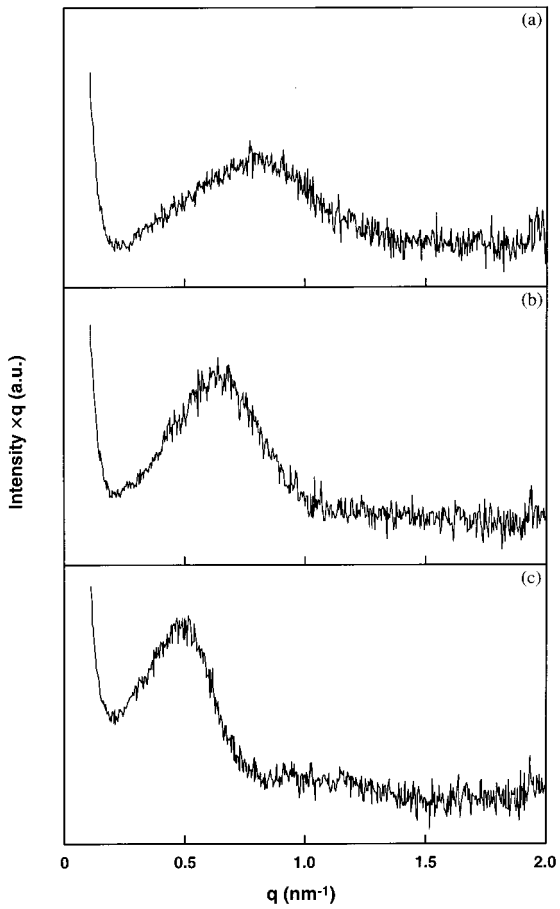

Figure 2. Variation in small-angle X-ray scattering (SAXS) intensity with q for P[(*R*)-3HB-*co*-6 mol % (*R*)-3HV] films crystallized (a) 60, (b) 90, and (c) 120 °C.

thickness (l_c) of melt-crystallized copolymer samples are listed in Table 2. The L_p value of P[(*R*)-3HB] homopolymer increased from 7.4 to 12.1 nm as the crystallization temperature was increased from 60 to 130 °C. The l_c value of P[(*R*)-3HB] samples also increased from 5.3 to 8.2 nm with an increase in crystallization temperature. The L_p values of P[(*R*)-3HB-*co*-6 mol % (*R*)-3HV] and of P[(*R*)-3HB-*co*-16 mol % (*R*)-3HV] had ranges of 7.2−13.8 and 6.7−17.1 nm, respectively. The l_c values of P[(*R*)-3HB-*co*-6 mol % (*R*)-3HV] and of P[(*R*)-3HB-*co*-16 mol % (*R*)-3HV] ranged from 4.1 to 8.5 nm and from 4.0 to 10.8 nm, respectively. For the other copolyester samples, the L_p and l_c values ranged from 5.3 to 9.9 nm and from 1.6 to 3.5 nm, respectively, and both values tended to increase with the crystallization temperature. It is noted that the l_c values of copolyester samples except for P[(*R*)-3HB-*co*-(*R*)-3HV] copolymers were smaller than those of P[(*R*)-3HB] homopolymer samples. In contrast, the l_c values of P[(*R*)-3HB-*co*-(*R*)-3HV] copolymers were almost consistent with the value for the P[(*R*)-3HB] homopolymer at a given crystallization temperature. It has been well-known that the P[(*R*)-3HB-*co*-(*R*)-3HV] copolymers show the isodimorphism due to the cocrystallization of (*R*)-3HB and (*R*)-3HV units in the composition range from 0 to 30 mol % of (*R*)-3HV units.[24] The l_c data of copolyester samples in Table 2 suggest that a portion of (*R*)-3HV units is included into P[(*R*)-3HB] crystalline lattice, while the other second monomer units are excluded from the P[(*R*)-3HB] crystalline lattice.

The reduction in melting temperature from an equilibrium value is accounted for in terms of the limited

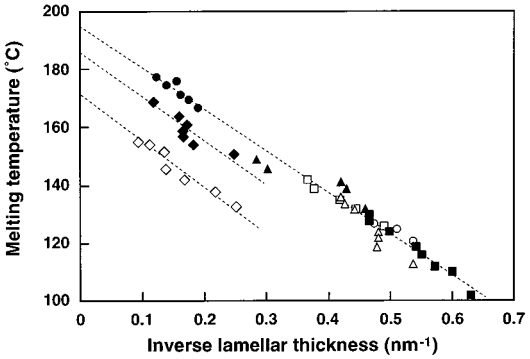

Figure 3. Variation in melting temperature (T_m) as a function of the inverse lamellar thickness ($1/l_c$) for melt-crystallized polyester films: (●) P[(*R*)-3HB]; (◆) P[(*R*)-3HB-*co*-6 mol % (*R*)-3HV]; (◇) P[(*R*)-3HB-*co*-16 mol % (*R*)-3HV]; (○) P[(*R*)-3HB-*co*-8 mol % (*R*)-3HH]; (▲) P[(*R*)-3HB-*co*-8 mol % 4HB]; (△) P[(*R*)-3HB-*co*-10 mol % 4HB]; (■) P[(*R*)-3HB-*co*-10 mol % 6HH]; (□) P[(*R*)-3HB-*co*-5 mol % LA].

lamellar thickness and may be expressed theoretically by the Gibbs-Thompson, equation, eq 1, where T_m is the

$$T_m = T_m^0\left(1 - \frac{2\sigma_e}{\Delta H_m l_c}\right) \quad (1)$$

observed melting temperature, T_m^0 is the equilibrium melting temperature, σ_e is the fold surface free energy, ΔH_m is the heat of fusion, and l_c is the lamellar thickness. Figure 3 shows the relationship between the inverse lamellar thickness ($1/l_c$) and the melting temperature (T_m) of melt-crystallized polyester samples. For P[(*R*)-3HB] homopolymer, the plot of melting temperature against inverse lamellar thickness shows the linear relationship. From the intercept of the line, we find that $T_m^0 = 194 \pm 6$ °C and from the slope that $\sigma_e/\Delta H_m = 1.51 \times 10^{-10}$ m, taking $T_m^0 = 467$ K. For P[(*R*)-3HB-*co*-(*R*)-3HV] samples, the lines shifted to lower melting temperatures at the same lamellar thickness with an increase in the (*R*)-3HV fraction. The T_m^0 and $\sigma_e/\Delta H_m$ values of copolymers with (*R*)-3HV fractions of 6 mol % and 16 mol % were $T_m^0 = 185$ °C, $\sigma_e/\Delta H_m = 1.67 \times 10^{-10}$ m and $T_m^0 = 172$ °C, $\sigma_e/\Delta H_m = 1.84 \times 10^{-10}$ m, respectively. It is of interest to note that the plots of T_m against $1/l_c$ for copolyester samples except for P[(*R*)-3HB-*co*-(*R*)-3HV] samples fitted with the line obtained from plotting the T_m and $1/l_c$ of P[(*R*)-3HB] samples extrapolated toward thinner lamellar thickness. This result indicates that the crystalline structure of lamellae for copolyesters except for P[(*R*)-3HB-*co*-(*R*)-3HV] is essentially the same as that for P[(*R*)-3HB] homopolymer.

It has been concluded from the result of Figure 3 that the randomly distributed second monomer units except for (*R*)-3HV in PHA copolyesters act as defects of P[(*R*)-3HB] crystal and are excluded from the P[(*R*)-3HB] crystalline lamellae. Consequently, the lamellar thickness of copolyesters except for P[(*R*)-3HB-*co*-(*R*)-3HV] thinned down with incorporation of noncrystallizable second monomer units into (*R*)-3HB sequences.

Enzymatic Degradability of Melt-Crystallized Polyester Films. The enzymatic hydrolysis of melt-crystallized copolyester films was carried out in 0.1 M potassium phosphate buffer (pH 7.4) containing PHB depolymerase (1.0 μg/mL) from *Alcaligenes faecalis* at 37 °C. Figure 4 shows the scanning electron micrographs (SEMs) of the surfaces of P[(*R*)-3HB-*co*-10 mol % 6HH] film before and after enzymatic degradation. Before enzymatic degradation, the surface of P[(*R*)-3HB-*co*-10 mol % 6HH] film was almost flat. After enzymatic degradation, the surface was apparently blemished with time by the action of PHB depolymerase, and the ringed texture of P[(*R*)-3HB-*co*-10 mol % 6HH] spherulites was detected. In addition, two different types of planes can be observed on the surface of P[(*R*)-3HB-*co*-10 mol % 6HH] spherulites after 0.5 h of enzymatic degradation. The smooth and rough planes exist mutually along the radial direction of spherulite. The band distance of spherulites determined from the SEMs of films after enzymatic degradation increased with an increase in the crystallization temperature, and the values were in good agreement with the values of band spacing determined from the optical micrographs of spherulites. A similar observation was also confirmed in the other polyester samples. Scandola [33] have reported that the similar ringed texture of P[(*R*)-3HB] spherulite could be observed on the surface of melt-crystallized film exposed in activated sludge. The banded morphology of spherulites is well-known to arise from the difference of orientation of crystalline axis due to twisting of lamellar crystals. Therefore, both chain-folding plane and crystal edge plane of lamellae appear on the surface of melt-crystallized polyester films. Hocking et al. [25] and Iwata et al. [26] have prepared single crystals of P[(*R*)-3HB] homopolymer and studied the enzymatic degradation of single crystals with bacterial PHB depolymerases. It has been concluded that the attack by the active site of PHB depolymerase takes place preferentially at the crystal edges rather than the chain-folding surfaces of single crystals. As it is shown in Figure 4, PHB depolymerase may predominantly hydrolyze the polymer chains at the crystal edge of lamellar stacks on the surface of melt-crystallized films.

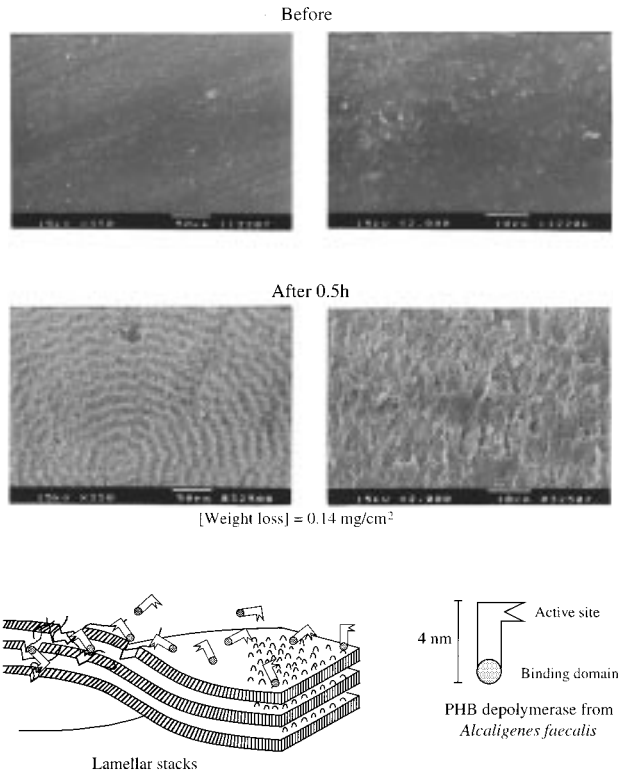

Figure 4. Scanning electron micrographs of the surfaces of P[(*R*)-3HB-*co*-10 mol % 6HH] film before and after enzymatic degradation for 0.5 h by PHB depolymerase from *A. faecalis*.

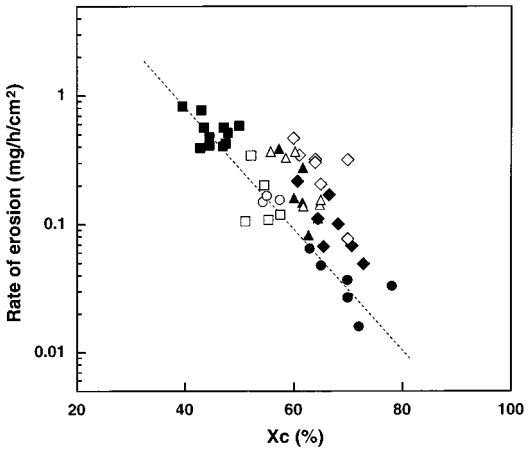

Figure 5. Relation between the rate of enzymatic erosion (R) and the degree of crystallinity (X_c) for melt-crystallized polyester films: (●) P[(*R*)-3HB]; (◆) P[(*R*)-3HB-*co*-6 mol % (*R*)-3HV]; (◇) P[(*R*)-3HB-*co*-16 mol % (*R*)-3HV]; (○) P[(*R*)-3HB-*co*-8 mol % (*R*)-3HH]; (▲) P[(*R*)-3HB-*co*-8 mol % 4HB]; (△) P[(*R*)-3HB-*co*-10 mol % 4HB]; (■) P[(*R*)-3HB-*co*-10 mol % 6HH]; (□) P[(*R*)-3HB-*co*-5 mol % LA].

The rate of enzymatic erosion was determined from the slope of line plotting the weight loss against reaction time, and the data are listed in Table 2. Figure 5 shows the relationship between the rate of enzymatic erosion and degree of crystallinity of melt-crystallized polyester films. The rate of enzymatic erosion of melt-crystallized polyester films decreased from 0.840 mg/(h/cm^2) to 0.016 mg/(h/cm^2) as the degree of crystallinity was increased from 40% to 78%. It has been reported that PHB depolymerase initially hydrolyzes amorphous P[(*R*)-3HB] chains on the surface and subsequently erodes the polymer chains in the crystalline state.[15−17] In addition, the rate of enzymatic hydrolysis for polyester chains in amorphous region has been found to be much faster than that in crystalline region.[15] Then, a decrease in the enzymatic erosion rate of melt-crystallized copolyester film with crystallization temperature may be caused by an increase in the crystallinity. However, it is noted from the result of Figure 4 that the rates of enzymatic erosion for the P[(*R*)-3HB-*co*-(*R*)-3HV] films are several times higher than those of P[(*R*)-3HB] films, when the rates are compared with those for films of an identical crystallinity. The significant difference in the erosion rates for melt-crystallized films of P[(*R*)-3HB] homopolymer and P[(*R*)-3HB-*co*-(*R*)-3HV] copolymers could not be explained only in terms of degree of crystallinity.

The film erosion by enzymatic hydrolysis is composed of the erosions on both crystalline and amorphous phases. It is well-known that the PHB depolymerase hydrolyzes the polyester chains on the surface of film, and that the weight loss of film by enzymatic erosion increases proportionally with reaction time.[16, 17] It is apparent that the enzymatic degradation in amorphous and crystalline phases occurs alternately from the surface of film, since the film thickness decreased with time. Therefore, the overall rate of film erosion (R) may be expressed by the erosion rates of crystalline (R_c) and amorphous (R_a) phases with the degree of crystallinity (xc) as eq 2.

$$\frac{1}{R} = \frac{x_c}{R_c} + \frac{1 - x_c}{R_a} \quad (x_c = X_c/100) \tag{2}$$

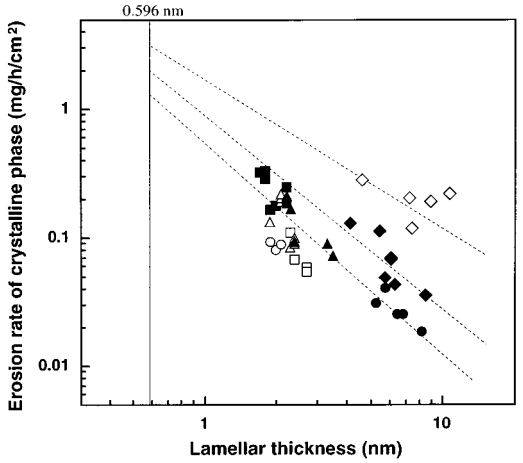

Figure 6. Relationship between the erosion rate of crystalline phase (R_c) and the lamellar thickness (l_c): (●) P[(*R*)-3HB]; (◆) P[(*R*)-3HB-*co*-6 mol % (*R*)-3HV]; (◇) P[(*R*)-3HB-*co*-16 mol % (*R*)-3HV]; (○) P[(*R*)-3HB-*co*-8 mol % (*R*)-3HH]; (▲) P[(*R*)-3HB-*co*-8 mol % 4HB]; (△) P[(*R*)-3HB-*co*-10 mol % 4HB]; (■) P[(*R*)-3HB-*co*-10 mol % 6HH]; (□) P[(*R*)-3HB-*co*-5 mol % LA].

In previous papers,[8−12] enzymatic degradabilities of microbial and chemosynthetic PHA films by PHB depolymerase have been investigated, suggesting that the *endo* cleavage of PHA chains by PHB depolymerase occurs together with *exo* cleavage. In this study, we used the random copolymers with second monomer compositions ranging in 6−16 mol % to minimize the effect of copolymer composition on the hydrolysis of polymer chain. As shown in Table 2, the rates of film erosion of P[(*R*)-3HB-*co*-10 mol % 6HH] samples with 40−50% crystallinity (0.396−0.840 mg/h/cm^2) were several decades times larger than those of P[(*R*)-3HB] samples with 63−78% crystallinity (0.016−0.066 mg/h/cm^2). This result indicates that the erosion rate of amorphous phase (R_a) is much larger than that of crystalline phase (R_c). Under the condition that $R_a \gg R_c$, the erosion rate of crystalline phase is approximated for melt-crystallized polyester films over 40% crystallinity by the product of the overall rate of film erosion and degree of crystallinity.

$$\frac{1}{R} = \frac{x_c}{R_c}, \quad R_c = x_c R \tag{3}$$

The R_c values of melt-crystallized polyester films varied from 0.012 to 0.336 mg/h/cm^2 with varieties of polyesters and crystallization temperatures, suggesting that the difference in R_c value arises from the difference in crystal dimension such as crystal size and lamellar thickness. In fact, the rate of enzymatic erosion of melt-crystallized P[(*R*)-3HB] films with PHB depolymerase was reported to be affected by the P[(*R*)-3HB] crystal size.[16] As shown in Figure 4, enzymatic hydrolysis of polymer chains in the crystalline phase takes place from the edge of P[(*R*)-3HB] crystal, rather than from the fold surface.

Here, we point out that the erosion rate of crystalline phase is strongly dependent on the lamellar thickness. Figure 6 shows the relationship between the erosion rate of crystalline phase (R_c) and lamellar thickness (l_c) of melt-crystallized copolyester films. The erosion rate of crystalline phase in melt-crystallized films increased markedly with a decrease in the lamellar thickness. However, it is noted from Figure 6 that the erosion rates

of crystalline phase in P[(*R*)-3HB-*co*-(*R*)-3HV] films are several times higher than those of P[(*R*)-3HB] films of an identical lamellar thickness and increase with an increase in the (*R*)-3HV fraction.

It is well-known that PHB depolymerase has a binding domain to adhere to hydrophobic substrates such as the surface of P[(*R*)-3HB], in addition to a catalytic domain as a active site.[27−29] The enzymatic erosion of P[(*R*)-3HB] film takes place via two steps, namely, adsorption and hydrolysis; the first step is adsorption of the enzyme on the surface of P[(*R*)-3HB] film by the binding domain of enzyme, and the second step is a hydrolysis of the polymer chains by the active site of enzyme.[30] PHB depolymerase adheres to the surface of crystalline lamellae of P[(*R*)-3HB], while it hardly binds with polymer chains in an amorphous phase.[31,32] The binding of PHB depolymerase on the edge of P[(*R*)-3HB] lamellar crystal may cause an increase in the mobility of polyester chains along the crystal edge, resulting in the formation of disordered P[(*R*)-3HB] chains such as polymer chains in amorphous phase which are facilely attacked by the active site of enzyme. The polyester chains exposed on the edge of relatively thin crystalline lamellae may more easily form the disordered polyester chains, rather than those on the edge of relatively thick crystalline lamellae. As a result, the erosion rate of crystalline phase may increase with a decrease in lamellar thickness. In addition, the crystallizable chains of P[(*R*)-3HB-*co*-(*R*)-3HV] on the edge of crystalline lamellae may be more mobile than the chains of P[(*R*)-3HB] homopolymer on the crystal edge, since the melting temperatures of P[(*R*)-3HB-*co*-(*R*)-3HV] are lower than those of P[(*R*)-3HB] samples of an identical lamellar thickness. As a results, more facile erosion by PHB depolymerase may be observed on the isodimorphic crystals of P[(*R*)-3HB-*co*-(*R*)-3HV].

Conclusions

The lamellar crystal structures and thermal properties for melt-crystallized films of copolymers of (*R*)-3HB with different hydroxyalkanoic acids ((*R*)-3HV, (*R*)-3HH, 4HB, 6HH, and LA) were characterized by SAXS and DSC measurements. The relationship between lamellar thickness and melting temperature of PHA samples indicates that the randomly distributed second monomer units except for (*R*)-3HV in PHA copolymers act as defects of P[(*R*)-3HB] crystal and are excluded from P[(*R*)-3HB] crystalline lamellae. The enzymatic erosion rate of crystalline phase in the melt-crystallized PHA films by PHB depolymerase from *A. faecalis* markedly decreased with an increase in the lamellar thickness.

Acknowledgment. This work was supported by CREST (Core Research for Evolutional Science and Technology) of the Japan Science and Technology Corporation (JST).

References and Notes

(1) Holmes, P. A. In *Developments in Crystalline Polymers—2*; Bassett, D. C., Ed.; Elsevier: London, 1988: p 1.

(2) Doi, Y. *Microbial Polyesters*; VCH Publishers: New York, 1990.

(3) Anderson, A. J.; Dawes, E. A. *Microbiol. Rev.* **1990**, *54*, 450.

(4) Steinbüchel, A.; Valentin, H. E. *FEMS Microbiol. Lett.* **1995**, *128*, 219.

(5) Tanio, T.; Fukui, T.; Shirakura, Y.; Saito, T.; Tomita, K.; Kaiho, T.; Masamune, S. *Eur. J. Biochem.* **1982**, *124*, 71.

(6) Mukai, K.; Yamada, K.; Doi, Y. *Polym. Degrad. Stab.* **1993**, *41*, 85.

(7) Jendrossek, D.; Schirmer, A.; Schlegel, H. G. *Appl. Microbiol. Biotechnol.* **1996**, *46*, 451.

(8) Doi, Y.; Kanesawa, Y.; Kunioka, M.; Saito, T. *Macromolecules* **1990**, *23*, 26.

(9) Shimamura, E.; Scandola, M.; Doi, Y. *Macromolecules* **1994**, *27*, 4429.

(10) Doi. Y.; Kitamura, S.; Abe, H. *Macromolecules* **1995**, *28*, 4822.

(11) Abe, H.; Doi, Y.; Aoki, H.; Akehata, T.; Hori, Y.; Yamaguchi, A. *Macromolecules* **1995**, *28*, 7630.

(12) Abe, H.; Doi, Y.; Aoki, H.; Akehata, T.; Hori, Y.; Yamaguchi, A. *Polymer* **1997**, in print.

(13) Barham, P. J.; Keller, A.; Otun, E. L.; Holmes, P. J. *J. Mater. Sci.* **1984**, *19*, 2781.

(14) de Koning, G. J. M.; Scheeren, A. H. C.; Lemstra, P. J.; Peeters, M.; Reynaers, H. *Polymer* **1994**, *35*, 4598.

(15) Kumagai, Y.; Kanesawa, Y.; Doi, Y. *Makromol. Chem.* **1992**, *193*, 53.

(16) Tomasi, G.; Scandola, M.; Briese, B. H.; Jendrossek, D. *Macromolecules* **1996**, *29*, 507.

(17) Koyama, N.; Doi, Y. *Macromolecules* **1997**, *30*, 826.

(18) Doi, Y.; Tamaki, A.; Kunioka, M.; Soga, K. *Appl. Microbiol. Biotechnol.* **1988**, *28*, 330.

(19) Nakamura, S.; Doi, Y.; Scandola, M. *Macromolecules* **1992**, *25*, 4237.

(20) Shirakura, Y.; Fukui, T.; Saito, T.; Okamoto, Y.; Narikawa, T.; Koide, K.; Tomita, K.; Takemasa, T.; Masamune, S. *Biochim. Biophys. Acta* **1986**, *880*, 46.

(21) Vonk, C. G. *J. Appl. Crystallogr.* **1973**, *6*, 148.

(22) Vonk, C. G. *J. Appl. Crystallogr.* **1975**, *8*, 340.

(23) Verma, R.; Marand, H.; Hsiao, B. *Macromolecules* **1996**, *29*, 7767.

(24) Bloembergen, S.; Holden, D. A.; Hamer, G. K.; Bluhm, T. L.; Marchessault, R. H. *Macromolucules* **1986**, *19*, 2865.

(25) Hocking, P. J.; Marchessault, R. H.; Timmins, M. R.; Lenz, R. W.; Fuller, R. C. *Macromolecules* **1996**, *29*, 247.

(26) Iwata, T.; Doi, Y.; Kasuya, K.; Inoue, Y. *Macromolecules* **1997**, *30*, 833.

(27) Saito, T.; Suzuki, K.; Yamamoto, J.; Fukui, T.; Miwa, K.; Tomita, K.; Nakanishi, S.; Odani, S.; Suzuki, J.; Ishikawa, K. *J. Bacteriol.* **1989**, *171*, 184.

(28) Jendrossek, D.; Müller, B.; Schlegel, H. G. *Eur. J. Biochem.* **1993**, *218*, 701.

(29) Jendrossek, D.; Frisse, A.; Behrends, A.; Andermann, M.; Kratzin, H. D.; Stanislawski, T.; Schlegel, H. G. *J. Bacteriol.* **1995**, *177*, 596.

(30) Kasuya, K.; Inoue, Y.; Doi, Y. *Int. J. Biol. Macromol.* **1996**, *19*, 35.

(31) Abe, H.; Matsubara, I.; Doi, Y. *Macromolecules* **1995**, *28*, 844.

(32) Scandola, M.; Focarete, M. L.; Adamus, G.; Sikorska, W.; Baranowska, I.; Swieczek, S.; Gnatowski, M.; Kowalczuk, M.; Jedlinski, Z. *Macromolecules* **1997**, *30*, 2568.

(33) Scandola, M. *Can. J. Microbiol.* **1995**, *41 (Suppl. 1)*, 310.

MA971559V